Efficient, accurate and flexible Finite Element solvers for Chemotaxis problems

Robert Strehl*, Andriy Sokolov*, Stefan Turek*

Abstract

In the framework of Finite Element discretizations we introduce a fully nonlinear Newton-like method and a linearized second order approach in time applied to certain partial differential equations for chemotactic processes incorporating two entities, a chemical agent and the reacting population of certain biological organisms/species. We investigate the benefit of a corresponding monolithic approach and the decoupled variant. In particular we analyze accuracy, efficiency and stability of the different methods and their dependencies on certain parameters in order to identify a well suited Finite Element solver for chemotaxis problems.

Keywords: chemotaxis model, pattern formation, finite element, Newton, monolithic, nonlinear

1. Introduction

This current work deals with systems of partial differential equations (PDEs) that describe a phenomenon that enables organisms to sense chemical signals and eventually encourages them to approach or avoid these signals. This ability is termed *chemotaxis* and serves the organisms in a wide range of objectives, such as localizing food sources, sexual partners, predators and toxic substances. Chemotaxis even can be used for communication-like purposes. The latter is the background of the PDE models that are applied in this present investigation. Communication among a culture of living organisms plays a key-role in their life-cycles, because it triggers the development of differentiated stadiums, e.g. aggregation in general or formation of slime-mold spores as in the life-cycle of *Dictyostelium discoideum.* Indeed the formation of certain structures can numerically nicely be obtained by considering particular models of chemotaxis, see the references that will be given in the corresponding context in section 2 and 4. Hence, chemotaxis is a major biological property and is worth its numerical investigation.

Up to the present, many scientists encouraged themselves in modeling complex chemotaxis systems of PDEs by introducing kinetic terms, incorporating certain quorum-sensing or volume-filling mechanisms or even extend the system to multiple species/ chemical agents. However most of this research lacks of a very important issue, the

*Institut für Angewandte Mathematik, TU Dortmund, E-mail addresses: robert.strehl@math.uni-dortmund.de, asokolow@math.uni-dortmund.de, ture@featflow.de.

implementation of a numerically well elaborated solver. From numerical point of view this is far from being trivial. Already established analytical results to certain chemotaxis models revealed the urgent needs of a numerical solver that captures solutions of very small support (e.g. in the case of *blowing up solutions*) or thin layered interfaces (e.g. in the case of *aggregating* or *pattern-forming solutions*). Only in the last couple of years researchers also began to consider the numerical treatment of such models by using different numerical approaches, such as Finite Element (FE), Finite Volume, discontinuous Galerkin or Finite Differences. However, up to now, corresponding numerical results have never been related to each other. That is, a quantitative comparison of different numerical approaches in the realm of chemotaxis PDEs have never been carried out. This numerical gap becomes even more crucial when considering the big effort that is exerted in the theoretical investigation of more and more complex chemotaxis PDEs.
This paper represents an attempt to gain first insights into the numerical applicability (efficiency) of different numerical schemes for chemotaxis PDEs. In particular we investigate FE algorithms with three different complexities by applying them on some typical chemotaxis models. These benchmarking models represent situations of aforementioned (numerically) crucial properties of solutions (blowing-up, aggregation and pattern-forming).

The present paper can be outlined as follows. After this opening section we will introduce a general PDE for chemotaxis and three particular models, which are derived from the general formulation and serve us as exemplary benchmarks. Based on these models the three underlying numerical schemes are presented in the third section and we will roughly sketch their basic properties in terms of pros and cons. The main part of this current work is investigated in section four. Therein we study the numerical applicability of the previously illustrated schemes. After concluding our results, the last section is dedicated to some further remarks and discussions.

2. The chemotaxis models

In this present paper we consider three particular systems of PDEs that model chemotactical dynamics. All of these models can be derived from a more generic form of chemotaxis PDEs. For a two dimensional domain $\Omega \subset \mathbb{R}^2$ this generic form reads

$$\left\{\begin{array}{rl} \dfrac{\partial u}{\partial t} = & \nabla \cdot \big(\underbrace{\nabla u}_{\text{diffusion}} - \underbrace{u\,\chi(c)\,\nabla c}_{\text{chemotaxis}}\big) + \underbrace{g(u)\,u}_{\text{growth}} \qquad , \; x \in \Omega \quad , t > 0 \\ \dfrac{\partial c}{\partial t} = & \underbrace{d\,\Delta\,c}_{\text{diffusion}} - \underbrace{\beta\,c}_{\text{depletion}} + \underbrace{s(u)\,u}_{\text{production}} \qquad , \; x \in \Omega \quad , t > 0. \end{array}\right. \tag{1}$$

Here and hereafter $u(\boldsymbol{x}, t)$ denotes a cell density and $c(\boldsymbol{x}, t)$ is a chemoattractant concentration. A variety of models can now be derived by defining the generic coefficients $\chi(\cdot)$, $g(\cdot)$, d, β, $s(\cdot)$. The above system will be endowed with usual prescribed initial values

$$u|_{t=0} = u_0, \qquad c|_{t=0} = c_0 \qquad \text{in} \quad \Omega \tag{2}$$

and certain boundary conditions, e.g. homogeneous Neumann boundary conditions

$$\boldsymbol{n}\cdot\nabla u = 0 \qquad \boldsymbol{n}\cdot\nabla c = 0 \qquad \text{on} \quad \partial\Omega, \tag{3}$$

or total flux boundary conditions of the form

$$\boldsymbol{n}\cdot\big(\nabla u - \chi(c)\,\nabla c\big) = 0, \qquad \boldsymbol{n}\cdot\nabla c = 0 \qquad \text{on} \quad \partial\Omega, \tag{4}$$

where $\boldsymbol{n}$ denotes the outward unit-normal on the boundary $\partial\Omega$.

Keeping the generic form (1) in mind, we can present our three governing models by selecting the generic coefficients. Our first model is also referred to as the minimal model of chemotaxis, which can be derived from the Patlak-Keller-Segel model proposed by Patlak [24], Keller and Segel [13, 14] in the 1970's. Its non-dimensionalized form reads

$$\begin{cases} \dfrac{\partial u}{\partial t} = & \nabla\cdot\big(\nabla u - \chi u \nabla c\big) \qquad , \ x\in\Omega \quad , t>0 \\[2ex] \dfrac{\partial c}{\partial t} = & \Delta\, c - c + u \qquad\qquad , \ x\in\Omega \quad , t>0, \end{cases} \tag{5}$$

where $\chi \in \mathbb{R}$ is now a constant describing the so-called chemosensitivity of the species $u(\boldsymbol{x}, t)$. This system can be obtained from the generic model (1) by selecting the following coefficients:

$$\chi(c) = \chi, \quad g(u) = 0, \quad d = 1, \quad \beta = 1, \quad s(u) = 1$$

The chemosensitivity χ solely characterizes the possible existence or unboundedness of the solutions. In fact various authors proved certain dependencies of the existence of a solution and the value of χ. After ongoing (nonlinear) stability analysis by Nanjundiah [21] and the conjectures of Childress [5] or Childress and Percus [6], Nagai et al. [20] finally proved a first connection of the existence of a solution and the value of χ in the two dimensional case. For further historical landmarks in the context of theoretical analysis of the minimal model (5) we refer to the survey paper of Horstmann [12]. From the numerical point of view this model has been investigated via different approaches, e.g. Chertock and Kurganov [4], Filbet [10] or Strehl et al. [26],[27] considered finite volume or finite element schemes wherein Epshteyn [8] and Epshteyn and Kurganov [9] developed interior penalty/discontinuous Galerkin methods.

The second model we like to focus on in this current paper is a chemotaxis system which introduces a logistic-like growth term for the cell density equation. This additive term obviously violates the mass conservation in this equation and, hence, may be capable to model certain proliferation dynamics. The model reads

$$\begin{cases} \dfrac{\partial u}{\partial t} = & \nabla\cdot\big(\nabla u - \chi u \nabla c\big) + u^2(1-u) \qquad , \ x\in\Omega \quad , t>0 \\[2ex] \dfrac{\partial c}{\partial t} = & \Delta\, c - \beta c + u \qquad\qquad\qquad , \ x\in\Omega \quad , t>0. \end{cases} \tag{6}$$

Its derivation from the generic model (1) is easy to see when considering the following settings:

$$\chi(c) = \chi, \quad g(u) = u(1-u), \quad d = 1, \quad s(u) = 1$$

Kinetic models of such a kind were theoretically discussed e.g. by Aida et al. [1], Tello and Winkler [28] or Mimura and Tsujikawa [17]. The global existence of solutions of (6) mainly stems from the decaying part of the logistic source $u^2(1-u)$. Numerically kinetic chemotaxis models, such as (6), have been studied e.g. by Myerscough et al. [19], Painter and Hillen [22] or Strehl et al. [26],[27]. Other authors investigated modifications of system (6), where they introduced volume-filling effects or additional equations, for instance in [4],[15],[23] or [30].

The last chemotactical system of PDEs that we consider in the present paper models an alternative to quorum sensing effects. In essence the nonlinear coefficients introduce certain Monod-like relations which conserve global existence of solutions. We will study the following aggregation model

$$\begin{cases} \dfrac{\partial u}{\partial t} = & \nabla \cdot \big(\nabla u - \chi \dfrac{u}{(1+c)^2} \nabla c\big) \qquad , \; x \in \Omega \quad , \; t > 0 \\[2ex] \dfrac{\partial c}{\partial t} = & d \, \Delta \, c + \dfrac{u^2}{1+u^2} \qquad\qquad\quad , \; x \in \Omega \quad , \; t > 0. \end{cases} \tag{7}$$

Note that we face a conservative equation for u (providing suitable zero total flux boundary conditions, cf. (4)) and no depletion terms in the c equation. System (7) can be obtained from the generic form (1) by choosing the following coefficients:

$$\chi(c) = \chi/(1+c)^2, \quad \beta = 0, \quad s(u) = u/(1+u^2)$$

In contrast to the preceding two models, system (7) introduces nonlinear terms in both equations. For the origin of those nonlinear terms the interested reader may be referred to the survey paper of Gerber [11] and the complementary references therein. Moreover Painter and Hillen [23] provide a good reference for quorum sensing (and volume filling) effects of chemotaxis models. Therein the authors considered a chemosensitivity function which was originally introduced by Segel in [25] and also appears in (7). Numerically the aggregation model (7) has already been studied by Chertock and Kurganov in [4] and Strehl et al. in [26] and [27].

These three models serve us as benchmarking systems for our nonlinear schemes which will be introduced in the proceeding section. However let us remark that our schemes may also be applicable to more comprehensive models, incorporating non-constant coefficients also for the diffusion-rates, different source-terms or even more equations (haptotaxis/ angiogenesis or in general multi-species models).
Furthermore, although the three governing models have already been studied numerically by different authors, the current paper presents, to the best of our current knowledge, first quantitative results for different solvers, rather than focusing solely on specific properties, e.g. positivity preservation, of particular finite difference/volume/element schemes.

3. The numerical schemes

For a brief reminder of the notation for a FE discretization, let us recall some FE basics which will be used for the remainder of this work:
Let $\Omega \in \mathbb{R}^2$ be the computational domain, with boundary denoted by $\partial\Omega$. In the present paper we only use quadratic domains and hence our spatial mesh can be constructed in a canonical equidistant fashion. That is, we use quadrilateral elements with uniform width δh. The underlying temporal grid $[0, T]$ will also have a uniform step size δt. The Galerkin discretization is now established by multiplying the PDE by a suitable test function and integrating the equation over Ω — the proceeding numerical results where obtained by using Q_1 as test- (and trial-) function space. For the temporal discretization we choose the common θ-scheme, which includes a fully explicit scheme (*forward Euler*) for $\theta = 0$ and a fully implicit scheme (*backward Euler*) for $\theta = 1$.
For convenience let us denote discrete variables, such as FE-matrices and vectors in bold letters. Also let a subscript denote the evaluation at the related timestamp, e.g. $u_n = u(t_n) = u(n \cdot \delta t)$, and a superscript mark the state of the variable at the related general iteration step, e.g. in a nonlinear iteration loop (e.g. cf. algorithm 2).
Let us assume a system of basis functions $\{\varphi_i\}_i$ for the underlying FE-space — in our case of Q_1 these functions are simple hat functions. After discretization in space the discrete Laplacian, the mass matrix and the coefficients of our generic model (1) result in the following FE-matrices

$$\begin{aligned}
\boldsymbol{M}_{ij} &= \int_\Omega \varphi_i \, \varphi_j \, \mathrm{d}\boldsymbol{x}, \\
\boldsymbol{L}_{ij} &= \int_\Omega \nabla\varphi_i \cdot \nabla\varphi_j \, \mathrm{d}\boldsymbol{x}, \\
\boldsymbol{K}_{ij}(c) &= \int_\Omega \chi(c) \, (\nabla c \cdot \nabla\varphi_i) \, \varphi_j \, \mathrm{d}\boldsymbol{x}, \\
\boldsymbol{G}_{ij}(u) &= \int_\Omega g(u) \, \varphi_i \, \varphi_j \, \mathrm{d}\boldsymbol{x}, \\
\boldsymbol{S}_{ij}(u) &= \int_\Omega s(u) \, \varphi_i \, \varphi_j \, \mathrm{d}\boldsymbol{x}.
\end{aligned} \tag{8}$$

Note that for $\boldsymbol{L}$ and $\boldsymbol{K}$ we applied the divergence theorem (in correspondance to the underlying boundary conditions, cf. (3) or (4)) to shift the gradient to the test function-space.

3.1. Decoupled approach

When considering a coupled system of PDEs such as (1), a first concern might be to what extend the cross-dependencies, e.g. the chemotaxis and production-rate terms, influence the solution of a numerical scheme. Maybe the coupling can practically be tackled in a segregated fashion. Therefore our first approach will be a standard decoupled scheme.

When discretizing system (1) in space via the method of FE and employing a certain temporal discretization, e.g. the θ-scheme we can simply decouple the system by means of using already computed solutions in the cross-dependending terms. Particularly if we choose first to solve for the chemoattractant c and then use the updated solution of c to solve for the cells u, we can depict the scheme for the generic model (1) as in the following algorithm 1.

We observe that even in the implicit case ($\theta = 1$) the whole scheme can only be considered as semi-implicit (because of the explicit treatment of the cross-dependencies). Theoretically the quality of this approach clearly depends on the strength of chemosensitivity and production rate, since they may also be viewed as the major indicator of the coupling for this model. Although this scheme seems to be unnatural (caused by the artificial decoupling), a practical advantage is the quasi-linearity of the resulting equations, which may decrease the overall computational costs and hence increase the efficiency. Furthermore note that the system matrix of the c-equation can be globally built outside the time step loop to save even more computational costs.

Algorithm 1 Decoupled approach

```
 1: for time step $n \leftarrow 0, n_{max}$ do
 2:     solve for $\boldsymbol{c}_{n+1}$ (using $\boldsymbol{c}_n, \boldsymbol{u}_n$)
 3:         Build system matrix: $\boldsymbol{A} \leftarrow \boldsymbol{M} + \theta\,\delta t\,\{d\,\boldsymbol{L} + \beta\,\boldsymbol{M}\}$
 4:         Build RHS: $\boldsymbol{b}(\boldsymbol{c}_n, u_n) \leftarrow \boldsymbol{M}\,\boldsymbol{c}_n - (1-\theta)\,\delta t\,[d\,\boldsymbol{L} + \beta\,\boldsymbol{M}]\,\boldsymbol{c}_n + \delta t\,\boldsymbol{S}(\boldsymbol{u}_n)\,\boldsymbol{u}_n$
 5:         Solve $\boldsymbol{A}\,\boldsymbol{c}_{n+1} = \boldsymbol{b}(\boldsymbol{c}_n, \boldsymbol{u}_n)$
 6:     end solve
 7:     solve for $\boldsymbol{u}_{n+1}$ (using $\boldsymbol{c}_n, \boldsymbol{c}_{n+1}, \boldsymbol{u}_n$)
 8:         Build system matrix: $\boldsymbol{A}(\boldsymbol{u}_{n+1}) \leftarrow \boldsymbol{M} + \theta\,\delta t\,\{\boldsymbol{L} - \boldsymbol{K}(\boldsymbol{c}_{n+1})\} + \boldsymbol{G}(\boldsymbol{u}_{n+1})$
 9:         Build RHS: $\boldsymbol{b}(\boldsymbol{c}_n, \boldsymbol{u}_n) \leftarrow \boldsymbol{M}\,\boldsymbol{u}_n - (1-\theta)\,\delta t\,[\boldsymbol{L} - \boldsymbol{K}(\boldsymbol{c}_n) + \boldsymbol{G}(\boldsymbol{u}_n)]\,\boldsymbol{u}_n$
10:         Solve $\boldsymbol{A}(\boldsymbol{u}_{n+1})\,\boldsymbol{u}_{n+1} = \boldsymbol{b}(\boldsymbol{c}_n, \boldsymbol{u}_n)$
11:     end solve
12: end for
```

However, in contrast to the c-equation, which can be considered linear in c, we remark that the solver of the u-equation may have to face a nonlinearity caused by the discretized growth term $\boldsymbol{G}(\cdot)$. Thus for the pattern model this algorithm should incorporate a defect correction when solving for $\boldsymbol{u}_n$. Algorithm 2 sketches a common way to counter this nonlinearity. This algorithm will then substitute the command lines 7–11 in the decoupled algorithm 1. In contrast to the 'new' nonlinearity introduced by the pattern model, algorithm 1 handles the minimal and the aggregation model (5), (7) without exerting any nonlinear loop. However let us remark that the aggregation model is somehow stronger coupled, which is obviously caused by the order of nonlinearities in the model, e.g. the chemosensitivity and production rate. Therefore for large time steps we might expect a rather poor accuracy of algorithm 1 when it is applied on models such as (7). In the following, let us denote the decoupled method by `Dec`.

3.2. Monolithic approach

In the previous subsection we introduced a rather naive, but straightforward numerical treatment of the cross-dependencies of chemotaxis models. A slightly more elaborate

Algorithm 2 Defect correction (for $\boldsymbol{u}_n$)

```
Solve for $\boldsymbol{u}_n$ using $\boldsymbol{c}_{n-1}, \boldsymbol{c}_n, \boldsymbol{u}_{n-1}$ via defect correction:
Build RHS: $\boldsymbol{b}_n \leftarrow \boldsymbol{M}\,\boldsymbol{u}_{n-1} - (1-\theta)\,\delta t\,[\boldsymbol{L} - \boldsymbol{K}(\boldsymbol{c}_{n-1}) + \boldsymbol{G}(\boldsymbol{u}_{n-1})]\,\boldsymbol{u}_{n-1}$
Initialization $\boldsymbol{u}^0 \leftarrow \boldsymbol{u}_{n-1}$
for $k \leftarrow 0, k_{max}$ do
    Build system matrix: $\boldsymbol{A}(\boldsymbol{u}^k) \leftarrow [\boldsymbol{M} + \theta\,\delta t\,\{\boldsymbol{L} - \boldsymbol{K}(\boldsymbol{c}_n)\} - \boldsymbol{G}(\boldsymbol{u}^k)]$
    Calculate residual: $\boldsymbol{res}_n^k \leftarrow \boldsymbol{b}_n - \boldsymbol{A}(\boldsymbol{u}^k)$
    if (converged) then quit
    end if
    Solve $\boldsymbol{A}(\boldsymbol{u}^k)\,\hat{\boldsymbol{u}} = \boldsymbol{res}_n^k$
    Update defect corrected solution: $\boldsymbol{u}^{k+1} \leftarrow \boldsymbol{u}^k + \hat{\boldsymbol{u}}$
end for
```

but also natural approach will lead to a monolithic treatment of the system, e.g. we solve the chemotaxis system (1) simultaneously for c and u. The obvious benefit will be that we do not have to consider temporal biased uncertainties that are artificially caused by the numerical scheme, such as when employing a decoupled approach. Basically a monolithic system of equations for two unknowns $\boldsymbol{u}$ and $\boldsymbol{c}$ can be written in the general form

$$\boldsymbol{A}(\boldsymbol{x}_{n+1})\boldsymbol{x}_{n+1} \quad = \quad \boldsymbol{b}(\boldsymbol{x}_n), \tag{11}$$

wherein $\boldsymbol{x_n} = (\boldsymbol{u}_n, \boldsymbol{c}_n)$ is the FE block-solution vector. For our generic chemotaxis model (1) the system matrix and the right-hand side read

$$\begin{aligned}
\boldsymbol{A}(\boldsymbol{x}_{n+1}) \quad &= \quad \begin{bmatrix} \boldsymbol{M} + \theta\,\delta t\,\big\{\boldsymbol{L} - \chi\,\boldsymbol{K}(c_{n+1}) + \theta\,\delta t\,\boldsymbol{G}(u_{n+1})\big\} & \\ -\theta\,\delta t\,\boldsymbol{S}(u_{n+1}) & \boldsymbol{M} + \theta\,\delta t\,\big\{d\,\boldsymbol{L} + \beta\,\boldsymbol{M}\big\} \end{bmatrix}, \\
\boldsymbol{b}(\boldsymbol{x}_n) \quad &= \quad \begin{bmatrix} \boldsymbol{M}\boldsymbol{u}_n - (1-\theta)\,\delta t\,\big\{\boldsymbol{L} - \chi\,\boldsymbol{K}(\boldsymbol{c}_n) - \boldsymbol{G}(\boldsymbol{u}_n)\big\}\,\boldsymbol{u}_n \\ \boldsymbol{M}\boldsymbol{c}_n - (1-\theta)\,\delta t\,\big\{d\,\boldsymbol{L}\,\boldsymbol{c}_n + \beta\,\boldsymbol{M}\,\boldsymbol{c}_n + \boldsymbol{S}(\boldsymbol{u}_n)\,\boldsymbol{u}_n\big\} \end{bmatrix}.
\end{aligned}$$

Note that when choosing $\theta = 0$, e.g. employing *forward Euler*, the formulation (11) and the decoupled approach coincide, no matter which of the following two linearization techniques we apply.

3.3. Linearization techniques

The monolithic system (11) derived in the previous section includes nonlinear terms, e.g. $\boldsymbol{K}(\boldsymbol{c}_{n+1}), \boldsymbol{G}(\boldsymbol{u}_{n+1})$ and $\boldsymbol{S}(\boldsymbol{u}_{n+1})$. These nonlinearities may be tackled by different approaches. In the current paper we study two possible techniques, Newton-like methods and a linearization via extrapolation (in time). While a comprehensive numerical theory of the well known Newton method and its nonlinear loops can be found in e.g. [7], the latter tries to circumvent nonlinear iterations and was successfully applied in e.g. [29]. We will briefly introduce both methods and sketch their pros and cons from the theoretical point of view. A comparative numerical study will be presented later on in section 4.

3.3.1. Newton-like method

The basic idea of solving a nonlinear system like (11) via a Newton-like approach is to exert a iteration scheme for the solutions $\boldsymbol{x}^0, \boldsymbol{x}^1, \ldots, \boldsymbol{x}^m, \ldots$

$$\boldsymbol{x}^{m+1} \quad = \quad \boldsymbol{x}^m - \mathcal{F}_n(\boldsymbol{x}^m)^{-1} \boldsymbol{f}_n(\boldsymbol{x}^m). \tag{12}$$

Herein we define the residual as

$$\boldsymbol{f}_n(\boldsymbol{x}^m) \quad = \quad \boldsymbol{b}(\boldsymbol{x}_n) - \boldsymbol{A}(\boldsymbol{x}^m)\, \boldsymbol{x}^m, \tag{13}$$

and let $\mathcal{F}_n$ denote the Fréchet derivative of $\boldsymbol{f}_n$. Here and hereafter the sub-/superscript denotes the temporal/Newton iterate, respectively.
To circumvent the costly task to invert $\mathcal{F}_n$ in equation (12), we use the common workaround and solve the auxiliary equation

$$\mathcal{F}_n(\boldsymbol{x}^m)\, \boldsymbol{y} = -\boldsymbol{f}_n(\boldsymbol{x}^m). \tag{14}$$

After that we simply update our (previous) Newton iterate by means of

$$\boldsymbol{x}^{m+1} \quad = \quad \boldsymbol{x}^m + \boldsymbol{y}. \tag{15}$$

When implementing a Newton-like method there are certain issues which have to be kept in mind, such as: Does the local second order convergence of Newton's method pay off when considering the drawback of computational costs caused by derivation of the Jacobian? Do we want to calculate the exact Jacobian, or is it also feasible to approximate it (even use a preconditioner)? Do we solve the resulting linear sub-systems (14) exactly (e.g. via `UMFPACK`) or iteratively (e.g. via `BiCGStab`)? What kind of termination criterion shall we use? Which initial guess $\boldsymbol{x}^0$ should we use to ensure local high order convergence? Is there a need for a damping strategy to remain in the region of convergence?
This present paper only considers some particular configurations of Newton-like methods. For a thorough study of the general concept of different configurations we refer the interested reader to the literature, e.g. [7]. The configurations used in this investigation are as follows: We compute the exact Jacobian for model (5),(6) and a linearization for model (7) and solve the linear sub-systems iteratively via a stabilized `BiCGStab` solver [3]. In this current work we will use a pure residual based termination criterion (also called *affine contravariant* in the literature) which seems to work so far for our current models. As initial guess for the nonlinear iteration we choose the solution of the very previous time step and we do not exert a damping strategy yet since in our simulations the residuals practically decreased monotonically and rapidly enough.

For the sake of integrity let us state the (exact) Jacobian $\mathcal{F}_n = \mathcal{F}$ for the underlying models in the present paper — note that our Jacobian does not depend directly on the time step, therefore we drop the n index. We begin with the minimal model (5) and pattern model (6):

$$\mathcal{F}(\boldsymbol{x}^m) = \begin{bmatrix} -\boldsymbol{M} - \theta\,\delta t\left\{\boldsymbol{L} - \chi\,\boldsymbol{K}_1(\boldsymbol{c}^m) - \boldsymbol{G}_1(\boldsymbol{u}^m)\right\} & \theta\,\delta t\,\chi\,\boldsymbol{K}_2(\boldsymbol{u}^m) \\ \theta\,\delta t\,\boldsymbol{M} & -\boldsymbol{M} - \theta\,\delta t\left\{\boldsymbol{L} + \beta\,\boldsymbol{M}\right\} \end{bmatrix}, \tag{16}$$

where the three matrices $\boldsymbol{K}_1(\cdot)$, $\boldsymbol{K}_2(\cdot)$ and $\boldsymbol{G}_1(\cdot)$ are defined as follows

$$\begin{aligned}
\boldsymbol{K}_{1_{ij}}(c) &= \int_\Omega (\nabla c \cdot \nabla \varphi_i)\, \varphi_j \,\mathrm{d}\boldsymbol{x}, \\
\boldsymbol{K}_{2_{ij}}(u) &= \int_\Omega (\nabla \varphi_i \cdot \nabla \varphi_j)\, u \,\mathrm{d}\boldsymbol{x}, \\
\boldsymbol{G}_{1_{ij}}(u) &= \int_\Omega (2u - 3u^2)\, \varphi_i\, \varphi_j \,\mathrm{d}\boldsymbol{x}.
\end{aligned}$$

Note that for our minimal model $\boldsymbol{G}_1(\cdot)$ vanishes and $\beta = 1$.

When considering our third model (7) the modifications of the Jacobian are non-trivial, since the nonlinear contributions to the Jacobian will eventually inhibit a matrix representation as in (16). Therefore we propose a linearization of certain nonlinear terms in (7) via the well known Taylor expansion. Particularly we focus on the chemosensitivity function $\chi(c) = 1/(1+c)^2$ and on the total chemical production rate $s(u)\,u = u^2/(1+u^2)$. Consider the solutions u, c to be sufficient smooth, by Taylor expansion we obtain

$$\begin{aligned}
\chi(c+\varepsilon) &= \chi(c) - \frac{2}{(1+c)^3}\,\varepsilon + \mathcal{O}(\varepsilon^2), \\
s(u+\varepsilon)\,(u+\varepsilon) &= s(u)\,u - \Big(\frac{2u}{1+u^2} - \frac{2u^3}{(1+u^2)^2}\Big)\,\varepsilon + \mathcal{O}(\varepsilon^2).
\end{aligned}$$

Dropping the second order terms $\mathcal{O}(\varepsilon^2)$ and plugging these Taylor linearizations into the derivation of the Jacobian, we preserve the matrix representation and thus our Jacobian for model (7) can be approximated by

$$\mathcal{F}(\boldsymbol{x}^m) \doteq \begin{bmatrix} -\boldsymbol{M} - \theta\,\delta t\,\big\{\boldsymbol{L} - \chi\,\boldsymbol{K}_3(\boldsymbol{c}^m)\big\} & \theta\,\delta t\,\chi\,\big\{\boldsymbol{K}_4(\boldsymbol{u}^m, \boldsymbol{c}^m) - \boldsymbol{K}_5(\boldsymbol{u}^m, \boldsymbol{c}^m)\big\} \\ \theta\,\delta t\,\boldsymbol{S}_1(\boldsymbol{u}^m) & -\boldsymbol{M} - \theta\,\delta t\,\big\{d\,\boldsymbol{L} + \boldsymbol{M}\big\} \end{bmatrix}.$$

Herein the newly introduced matrices $\boldsymbol{K}_3, \boldsymbol{K}_4, \boldsymbol{K}_5$ and $\boldsymbol{S}_1$ are defined as

$$\begin{aligned}
\boldsymbol{K}_{3_{ij}}(c) &= \int_\Omega \frac{1}{(1+c)^2}\,(\nabla c \cdot \nabla \varphi_i)\, \varphi_j \,\mathrm{d}\boldsymbol{x}, \\
\boldsymbol{K}_{4_{ij}}(u,c) &= \int_\Omega \frac{u}{(1+c)^2}\,(\nabla \varphi_i \cdot \nabla \varphi_j) \,\mathrm{d}\boldsymbol{x}, \\
\boldsymbol{K}_{5_{ij}}(u,c) &= \int_\Omega \frac{2u}{(1+c)^3}\,(\nabla c \cdot \nabla \varphi_i)\, \varphi_j \,\mathrm{d}\boldsymbol{x}, \\
\boldsymbol{S}_{1_{ij}}(u) &= \int_\Omega \Big(\frac{2u}{1+u^2} - \frac{2u^3}{(1+u^2)^2}\Big)\, \varphi_i\, \varphi_j \,\mathrm{d}\boldsymbol{x}.
\end{aligned}$$

Let us recapitulate the Newton-like method, which we will refer to as `Newt`, in algorithm (3) in its generalized form.

We remark that for a (more) sophisticated nonlinear PDE the derivation of its exact Jacobian (or even its linearization) may be very tedious, if possible at all. To counter this costly and sometimes hard task we now have a look on a different linearization technique.

Algorithm 3 Newton-like method

```
for time step $n \leftarrow 1, n_{max}$ do
    Build RHS: $\boldsymbol{b}(\boldsymbol{x}_n)$
    Initialization: $m \leftarrow 0$; $x^0 \leftarrow x_n$
    while $m \leq m_{max}$ and not converged do
        Build system matrix: $\boldsymbol{A}(\boldsymbol{x}^m)$
        Calculate residual: $\boldsymbol{res}_n^m \leftarrow \boldsymbol{b}_n - \boldsymbol{A}(\boldsymbol{x}^m)$
        Build Jacobian: $\mathcal{F}(\boldsymbol{x}^m)$
        Solve $\mathcal{F}(\boldsymbol{x}^m)\,\boldsymbol{y} = -\boldsymbol{res}_n^m$
        Update Newton solution: $\boldsymbol{x}^{m+1} \leftarrow \boldsymbol{x}^m + \boldsymbol{y}$
    end while
    Update solution: $\boldsymbol{x}_{n+1} \leftarrow \boldsymbol{x}^{m+1}$
end for
```

3.3.2. Linearization via Extrapolation

Besides the two approaches we considered so far (`Dec` and `Newt`) there exists another commonly implemented method, the linearization via extrapolation. In principle this method takes the monolithic system matrix as introduced in (11). But in contrast to the Newton-like methods we directly linearize the nonlinear contributions in this system matrix in order to obtain an overall linearized system, e.g. we do not exert a nonlinear loop.

The idea of this linearization technique stems from an observation of the Taylor expansion of a sufficient smooth function. Let $f(t)$ be such a function and let $\{t_0, t_1, t_2, \dots\}$ with an uniform step width $\delta t = t_n - t_{n-1}$ be a discrete subset of the domain of f. We can now use a combination of two Taylor expansions to obtain an $\mathcal{O}(\delta t^2)$ approximation of $f(t_{n+1})$ only using the values $f(t_{n-1}), f(t_n)$. To this end we expand f centered at t_n and evaluate it at t_{n+1} and t_{n-1}:

$$+\left\{\begin{array}{lcl} T^f_{t_n}(t_{n+1}) & = & f(t_n) + f'(t_n)(t_{n+1} - t_n) + \mathcal{O}(\delta t^2) \\ \qquad\qquad T^f_{t_n}(t_{n-1}) & = & f(t_n) - f'(t_n)(t_{n-1} - t_n) + \mathcal{O}(\delta t^2) \end{array}\right.$$

$$\Rightarrow \quad T^f_{t_n}(t_{n+1}) + T^f_{t_n}(t_{n-1}) \quad \doteq \quad 2\,f(t_n)$$

Since $T^f_{t_n}(t_{n+1})$ and $T^f_{t_n}(t_{n-1})$ are second order approximations of $f(t_{n+1})$ and $f(t_{n-1})$, respectively, we can deduce

$$f(t_{n+1}) \quad = \quad 2\,f(t_n) - f(t_{n-1}) + \mathcal{O}(\delta t^2). \tag{18}$$

Thus we obtain a second order linearization if our underlying function f is smooth enough (second order differentiable) and the time stepping δt is sufficiently small (to ensure the convergence of the Taylor series expansion $T^f_{t_n}$).

It is now easy to apply this linearization to our governing model (1). For this general model of chemotaxis we have to modify the contribution of the chemosensitivity, chemical production rate and of the possible growth term in the system matrix $\boldsymbol{A}(\boldsymbol{x}_{n+1})$ in equation (11), we substitute the nonlinearity $\boldsymbol{c}_{n+1}, \boldsymbol{u}_{n+1}$ by the linearization

$2\,\boldsymbol{c}_n - \boldsymbol{c}_{n-1}, 2\,\boldsymbol{u}_n - \boldsymbol{u}_{n-1}$, respectively. Hence the (linearized) system matrix now reads

$$\boldsymbol{A}(\boldsymbol{x}_{n+1}) \quad \doteq \quad \begin{bmatrix} \boldsymbol{M} + \theta\,\delta t\left\{\boldsymbol{L} - \chi\,\boldsymbol{K}(2\,\boldsymbol{c}_n - \boldsymbol{c}_{n-1})\right\} & \theta\,\delta t\,\boldsymbol{G}(2\,\boldsymbol{u}_n - \boldsymbol{u}_{n-1}) \\ -\theta\,\delta t\,\boldsymbol{S}(2\,\boldsymbol{u}_n - \boldsymbol{u}_{n-1}) & \boldsymbol{M} + \theta\,\delta t\left\{d\,\boldsymbol{L} + \beta\,\boldsymbol{M}\right\} \end{bmatrix}.$$

Note that the right-hand side of (11) remains unchanged, since it represents no contribution to the nonlinearity. This linearization technique may also be viewed as an explicit two-step method, since the possible implicit character of the θ-scheme expires by the use of two priori computed solutions. For the remainder of this paper let `Lin` denote the linearized method, which can be summarized as in algorithm 4.

The pros of this method are that it works without any nonlinear iterations and it is second order accurate in time, in contrast to other linearization techniques e.g. the pure fixpoint method. However in contrast to the Newton-like methods it may provide poorer approximations/results at big time steps or in case of dominating nonlinearities.

Algorithm 4 Linearization via extrapolation

```
Initialization: $\boldsymbol{x}_n, \boldsymbol{x}_{n-1} \leftarrow \boldsymbol{x}_0$
for time step $n \leftarrow 1, n_{max}$ do
    Build RHS: $\boldsymbol{b}(\boldsymbol{x}_n)$
    Compute linearization: $\boldsymbol{x}_n^{lin} \leftarrow 2\,\boldsymbol{x}_n - \boldsymbol{x}_{n-1}$
    Build system matrix: $\boldsymbol{A}(\boldsymbol{x}_n^{lin})$
    Solve the linear System $\boldsymbol{A}(\boldsymbol{x}_n^{lin})\,\boldsymbol{x}_{n+1} = \boldsymbol{b}(x_n)$
end for
```

4. Numerical results

This section deals with the comparison of the three numerical schemes. The aim is to identify a measure of efficiency for the different approaches. Herein we understand efficiency as the ratio of accuracy and computational costs/complexity, e.g.

$$\text{efficiency} \quad = \quad \frac{\text{accuracy}}{\text{computational costs}} \quad .$$

While the accuracy will be measured by certain error-estimates, the computational costs will be mainly approximated by the entities of iterations that are exerted in the present algorithms. Although the authors are aware of the simplicity of these measures, they already lead to decent assertions.

On the one side the three schemes under consideration obviously have different general complexities. While the decoupled approach (`Dec`) and the Newton-like method (`Newt`) implement a nonlinear loop, the linearized scheme (`Lin`) cancelled out the nonlinearity. However the linearized scheme, as well as the Newton-like method, are based on a monolithic approach, e.g. they deal with block-vectors and -matrices. Therefore the complexity of their underlying solvers (e.g. `BiCGStab` or `UMFPACK`) is higher in comparison to the scalar-solvers for the decoupled approach. In table 1 we list the rough complexities of the three schemes. On the other side the accuracy of the schemes should also be considered. Clearly the implementation of a nonlinear loop and the utilization of a monolithic approach leads to a potentially more accurate solution in comparison to a linearized or decoupled/scalar approach.

Hence the question that certainly arises is to what extend the accuracy of the three schemes justifies their different complexities. In the current section we will present some fundamental quantitative results that help to identify the most favorable scheme for (each of the underlying) chemotaxis models.

	`Dec` $\star$	`Lin`	`Newt`
per time step	2 RHS 1 SOL	1 BLK-RHS 1 BLK-MAT 1 BLK-SOL	1 BLK-RHS
per nonlin. it.	1 MAT 1 SOL	–	2 BLK-MAT 1 BLK-SOL

Table 1: A rough sketch of the complexities for the three underlying schemes. RHS, MAT and SOL denote the right-hand side and matrix to be built and the call of the solver, respectively. BLK- represents the block-extensions for the monolithic approaches. ($\star$) The system matrix for the c-equation can be built globally, e.g. once at the beginning of the simulation.

4.1. Minimal model

At first we have a look on the applicability of the three approaches for the minimal model (5) with Neumann boundary conditions (3). The computational domain is the unit square $\Omega = (0,1)^2$, discretized via a uniform mesh size of $\delta h = 1/64$, e.g. 4096 quadrilaterals. We prescribe an analytic solution

$$u^*, c^* \quad = \quad \sigma_u \, 0.025(cos(2.0\pi(y-0.5)) + 1)(cos(2.0\pi(x-0.5)) + 1), \qquad (20)$$

which satisfies the Neumann boundary condition. We adapt our resulting system of fully discretized equations to this solution, by adding the contribution of (20) to the right-hand side. After prescribing an initial condition, we may run the 'pseudo time stepping' solver to reach its stationary limit. For this present study we use the following perturbed initial data

$$u_0, c_0 \quad = \quad (1 + \varepsilon \cdot \texttt{rand}) \, u^*, \qquad (21)$$

with ε being a perturbation scalar and `rand` representing a $(0,1)$-uniformly distributed random number.

In table 2 we depict the number of pseudo time steps that are needed to reach the stationary limit, e.g. the analytic given solution (up to a certain threshold), for different values of χ. For the time discretization we used the backward Euler, e.g. $\theta = 1$.

We observe that all three approaches behave similar for moderate values of χ. However for $\chi = 100$ the decoupled solver breaks down, as the number of nonlinear iterations (for solving for u) exceeds its limit (M_MAX). We conclude that the nonlinearity of the underlying minimal model is of moderate character, e.g. the fast decoupled approach is

χ	δt	`Dec`	`Lin`	`Newt`
1	1E-1	5	2	2
	1E-2	17	8	8
	1E-3	65	65	65
10	1E-1	5	2	2
	1E-2	17	8	8
	1E-3	72	68	68
50	1E-1	5	4	2
	1E-2	16	5	5
	1E-3	44	47	47
100	1E-1	M_MAX	4	2
	1E-2	M_MAX	6	6
	1E-3	48	50	50

Table 2: Iteration characteristics for the three approaches with **backward Euler** applied on the minimal model (5) where an analytic solution is prescribed. We depict the iterations needed to reach the approximated steady state reference solution (tolerance: 1E-6) with varying δt. We used `UMFPACK` as direct solver for the linear sub-problems. ε = -1E-5.

favorable for most configurations.
Let us remark that the defect correction introduced for the decoupled approach, algorithm 2, is indeed of linear character for the minimal model, since the term $\boldsymbol{G}(\cdot)$ vanishes. Furthermore we observed that the Newton-like method handled the nonlinear coupling with only one nonlinear iteration as well (except for $\chi = 100$).
Although we favor the decoupled approach for the pseudo time stepping, it is clear, that the monolithic treatment may give rise to a fully stationary solver. That is we solve the PDE (5) with $\partial u/\partial t = 0 = \partial c/\partial t$. In this case the Newton-like method turns out to be very efficient. Even for $\chi = 100$ the Newton-like stationary solver only requires two nonlinear iterations, whereas the decoupled variant and the linearized alternative need 48 and 50 pseudo time step iterations, respectively.
Let us finally remark, that (to a certain extend) all three schemes are capable to reproduce the setting of a blowing up or uniformly bounded solution, that are documented in e.g. [4], [9], [10], [26] and [27]. Due to the lack of stabilization techniques in our three underlying schemes, we will, however, not obtain new insights. Therefore we skip this setting and refer the interesting reader to the literature.

4.2. Aggregation model

While the minimal model mainly did not reveal big differences between the three approaches (for the pseudo time stepping), we now turn to the model (7), which introduces high(er)-order nonlinearities. We may expect these nonlinearities to reveal the benefits of the monolithic treatment against its decoupled counterpart, as already conjectured in the end of section 3.1.

Therefore let us consider model (7), again endowed with the Neumann boundary conditions (3), together with a random initial cell distribution:

$$\begin{array}{rcl} u_0(x) & = & 0.9 + 0.2 \cdot \texttt{rand} \\ c_0(x) & = & 0. \end{array} \qquad (22)$$

The basic parameter setting for this benchmark is $d = 0.33$ and $\chi = 80$. The underlying computational domain reads $\Omega = (0, 16)^2$ and is discretized with a mesh size of $\delta h = 0.25$, e.g. 4096 quadrilaterals. The time discretization is carried out with the Crank-Nicolson scheme, e.g. $\theta = 0.5$.
Already existing numerical approaches (for instance in [4, 26, 27]) revealed aggregating behavior of the cell distribution. That is single 'colonies of cells' merge together to form one larger colony. The aim under consideration is to investigate the development of the error to a pre-computed reference solution. Furthermore we conjecture a basic measurement for the quantification of the overall efficiency of the three numerical approaches. To this end the reference solution is computed via the Newton-like method on a very fine time stepping $\delta t =$ 1E-5 up to a certain timestamp $t_{end} = 0.3$. The error-estimates are then calculated for various time stepping δt and different values of χ.
Figure 1 depicts the initial condition (22) and the reference solutions. We notice that the aggregation behavior is influenced by χ, e.g. high values of χ trigger a more intense aggregation.

Figure 2 presents the errors for a sequence of decreasing time stepping δt. We observe that the decoupled approach leads to an error reduction of $\mathcal{O}(\delta t)$, whereas both monolithic approaches reveal an $\mathcal{O}(\delta t^2)$ decrease in the error (REF symbolizes the reference solution). For small δt this eventually induces an accuracy-gain of more than three digits for the monolithic approaches.

We may also study the overall efficiency of the different methods. To this end we may ask for the additional costs of the decoupled approach in order to obtain the accuracy of a simulation with one of the monolithic approaches. In particular we recognize the following for $\chi = 60$ (cf. figure 2 and table 3): Consider $\delta t =$ 1E-5 and $\delta t =$ 5E-4 for `Dec` and `Lin`, respectively. Even for a 50 times more accurate time discretization we cannot guarantee a similar error. Furthermore `Dec` requires an average of 73.7 iterations per time step for solving the sub-problem, whereas `Lin` only needs 37.8. This leads to an additional cost factor of approximately 100, e.g. in order to achieve a similar error (of $\approx$ 4.6E-6/1.3E-6), `Dec` requires 100 times more iterations than `Lin`. For `Dec` and `Newt` this 'ratio of efficiency' is about 200, cf. the data for $\delta t =$ 1E-5 and $\delta t =$ 2E-3, respectively. These ratios remain similar for $\chi = 80, 95$.

Hence the difference in the efficiency for the decoupled and the monolithic approaches is remarkable and we may obviously favor the monolithic variants for the aggregation model (7).

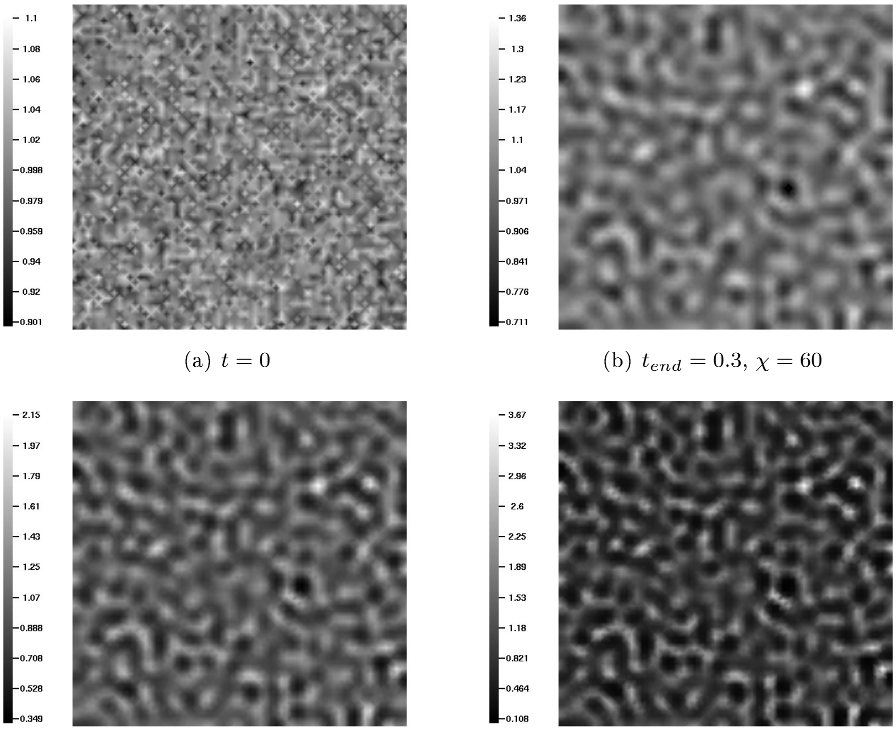

(a) $t = 0$

(b) $t_{end} = 0.3$, $\chi = 60$

(c) $t_{end} = 0.3$, $\chi = 80$

(d) $t_{end} = 0.3$, $\chi = 95$

Figure 1: Initial condition (22) and reference solutions of the aggregation model (7) for different values of χ.

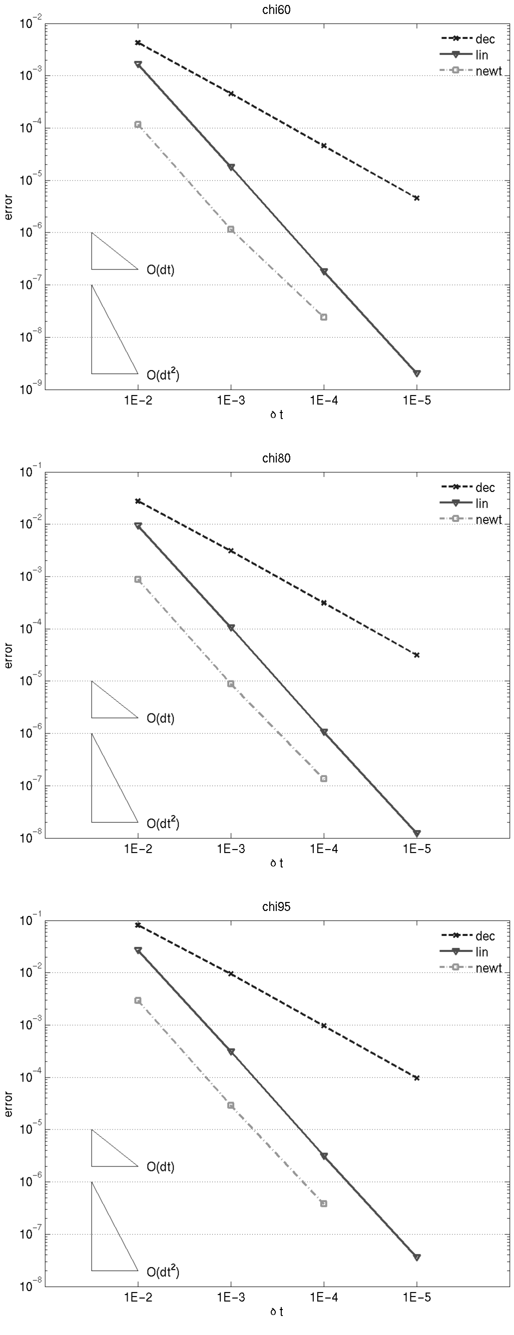

Figure 2: Relative error of `Dec`, `Lin` and `Newt` applied on the aggregation model (7) for $\chi =$ 60 (top) , 80 (mid) , 95 (bottom).

δt		Dec	Lin	Newt
$5E-2$	nonlin	-	-	3/3/3.0
	lin	16/16/16+19/21/20.5	22/24/23.0	30/41/35.2
$2E-2$	nonlin	-	-	2/3/2.7
	lin	22/23/22.1+17/19/18.0	21/24/22.9	26/32/28.9
$1E-2$	nonlin	-	-	2/3/2.0
	lin	28/28/28+22/25/22.8	24/30/27.0	26/39/31.6
$5E-3$	nonlin	-		2/2/2.0
	lin	32/32/32.0+28/32/28.9	31/34/32.1	27/41/33.3
$2E-3$	nonlin	-	-	2/2/2.0
	lin	34/35/34.0+33/39/34.7	34/39/36.1	30/43/35.1
$1E-3$	nonlin	-	-	2/2/2.0
	lin	35/36/35.0+34/42/37.3	36/41/37.4	31/42/35.8
$5E-4$	nonlin	-	-	2/2/2.0
	lin	36/36/36.0+34/43/38.8	36/43/37.8	32/43/36.9
$2E-4$	nonlin	-	-	1/2/1.4
	lin	36/37/36.0+34/44/39.2	37/46/38.0	33/45/36.7
$1E-4$	nonlin	-	-	1/2/1.0
	lin	36/37/36.0+34/43/39.0	37/46/38.5	33/49/36.9
$5E-5$	nonlin	-	-	1/1/1.0
	lin	36/38/36.1+34/43/38.4	38/47/39.0	33/49/37.1
$2E-5$	nonlin	-	-	1/1/1.0
	lin	36/38/36.3+34/44/37.6	38/46/39.6	33/51/36.8
$1E-5$	nonlin	-	-	1/1/1.0
	lin	36/38/36.4+35/44/37.3	37/46/40.0	33/51/37.7

Table 3: Iterations needed per time step for the three approaches applied on the aggregation model (7). Parameters as before, except $\chi = 60$. 'Nonlin' accounts for the minimal/maximal/average iterations of the nonlinear defect-correcting loop whereas 'lin' accounts analogously for the iterations of the linear sub-problem per nonlinear step. In the case of `Dec` we list the iterations for c and u, separated via $+$.

4.3. Pattern model

The last section revealed that high-order nonlinear terms in chemotaxis models give rise to a more comprehensively developed solver technique, whereas for the minimal model the simple decoupled approach already suffices. The pattern model (6) serves us as a third benchmarking model in order to investigate the applicability of the present three numerical methods. Therefore we now focus on the model (6) with the boundary conditions (3). The underlying computational domain is the square $\Omega = (0, 16)^2$. Initially we prescribe the following cell and chemical distributions

$$\begin{aligned} u_0(x) &= \begin{cases} 1 + 1.1\, cos^2(\pi\, r_{8,8}(x)) & \text{, for } r_{8,8}(x) \leq 1.5 \\ 1 & \text{, else} \end{cases} \\ c_0(x) &= 1/32, \end{aligned} \tag{23}$$

where $r_{8,8}(x)$ denotes the euclidian distance to the center of the domain $(8, 8)$.
It is well known that models like (6) exibit wave-like propagation throughout the whole domain, see the aforementioned literature. Particularly, it does not necessitate initial conditions with wave-characteristics as described in (23). This initial condition was only chosen for reproduction reasons. In figure 3 we plotted the initial condition (23) and the reference solutions for this set-up, which are obtained by `Newt` at the finest time stepping $\delta t =$ 1E-4 (for $\chi = 6$), 1E-5 (for $\chi = 8.5, 12$). We observe, that the wave-like propagation speed depends on χ, e.g. the propagation speed increases when χ increases.
As in the last section, in the following table and figures we present some error estimates for the three different numerical schemes applied to (6),(3),(23) with varying δt and χ. All simulations were driven up to a certain timestamp t_{end} with a time discretization via the Crank-Nicolson scheme, e.g. $\theta = 0.5$.
In contrast to the last section, now the numerical treatment of the underlying model involves nonlinear iterations also for the decoupled approach, note the presence of the $\boldsymbol{G}(\cdot)$ term in algorithm 2. This 'new' nonlinearity may enhance the overall efficiency of `Dec` in terms of smaller ratios concerning `Dec` and `Lin` or `Dec` and `Newt`.

Figure 5 displays the errors for a decreasing series of δt. As before, we obtain the $\mathcal{O}(\delta t)$ and $\mathcal{O}(\delta t^2)$ convergence for the decoupled and monolithic approach, respectively. Very roughly speaking this finally leads to an accuracy gain of four digits on the finest time stepping.

We observe certain problems for large time steps, which result in negative values or even a break-down of the solver. For $\chi = 8.5$ problems (in terms of negative values for $\delta t =$ 1E0) appear for the linearized approach only, but for $\chi = 12$ all solvers fail for large time steps, e.g. $\delta t =$ 1E0. While the decoupled solver exceeds its nonlinear iteration limit and the Newton-like method diverges (note the missing corresponding data in figure 5), the linearized method produces illusive solutions with negative values, see figure 4. When considering the situation that the exact solution is a-priori unknown, numerical methods reporting the break-down or divergence of the underlying solver are much more favorable than a method which produces a misleading output. Indeed when having a closer look on figure 5 we might only notice the problem for `Lin` when considering the poor convergence for $\delta t =$ 1E0,1E-1, particularly for $\chi = 12$.

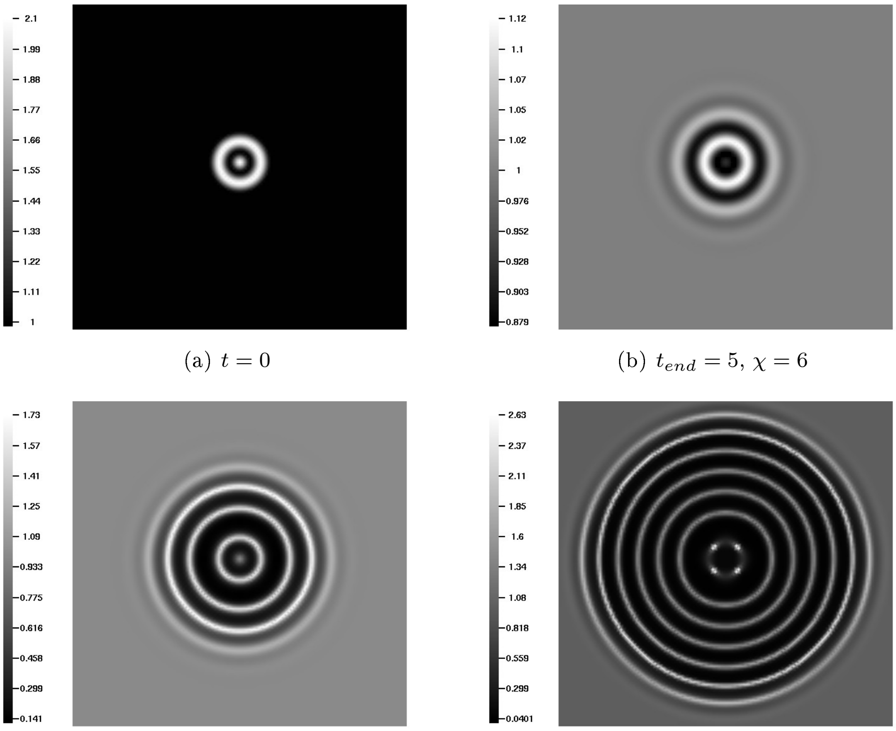

(a) $t = 0$

(b) $t_{end} = 5$, $\chi = 6$

(c) $t_{end} = 5$, $\chi = 8.5$

(d) $t_{end} = 5$, $\chi = 12$

Figure 3: Initial condition (23) and reference solutions of the pattern model (6) for different values of χ. Other parameters: $D_u = 0.0625, \alpha = 32$.

When having a look on the ratio of efficiency (as proposed in the preceding section) and focus on $\chi = 8.5$ (cf. figure 5 and table 4), we obtain the following: If we are asking for an error for `Dec` that is similar to the one obtained from `Lin` at δt = 1E-3 we have to refine the time stepping at least 100 times. Additionally the averaged iterations required by `Dec` and `Lin` are 54.8 and 27.6, respectively. This leads to an overall extra costs factor of approximately 200. When comparing `Dec` and `Newt` we similarly obtain a factor of more than 500, cf. the data for δt = 1E-5 and δt = 5E-3, respectively. Analogous results are obtained for $\chi = 6, 12$.
Another remarkable issue is that the averaged error-quotient of `Lin` (e_{Lin}) and `Newt` (e_{Newt}) at a fixed level of δt mostly increases when χ is increasing. That is, while the quotient at δt = 1E-3 is $e_{Lin}/e_{Newt} \approx 1.95$ for $\chi = 6$, it increases to 11.0 for $\chi = 8.5$ and finally reaches 14.7 for $\chi = 12$. In other words the χ-scaling stresses the accuracy of the Newton-like method.

In the end we can conclude that even if we consider a model which is only highly nonlinear in the u equation, for instance the present model (6), the decoupled approach looses its efficiency, in terms of overall invoked iterations. That is, although `Dec` introduces a nonlinear defect correction for u, the error of the artificial splitting of the

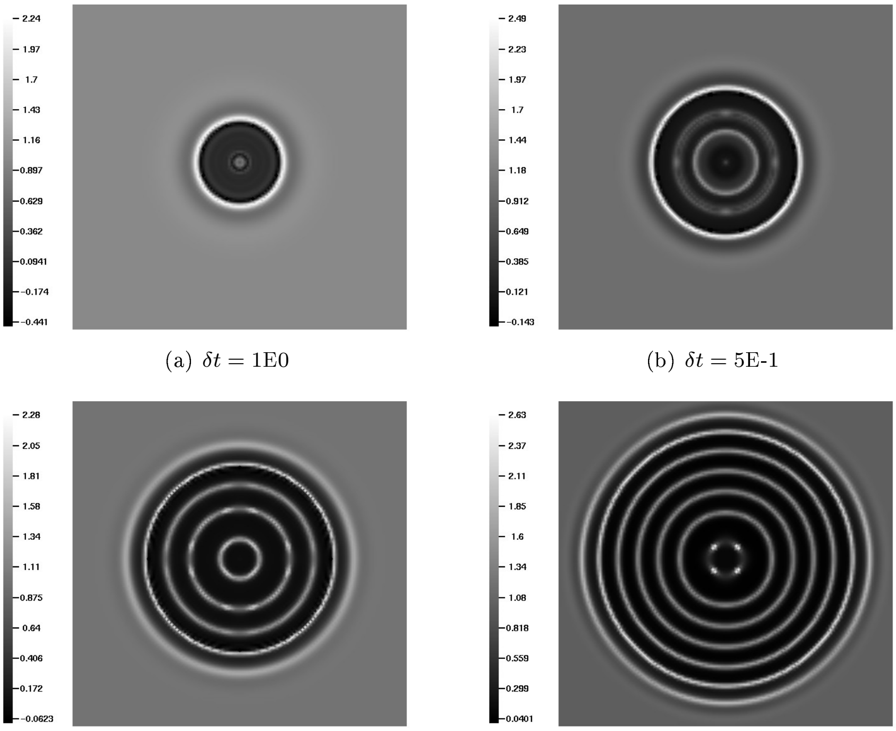

(a) $\delta t = 1\text{E}0$

(b) $\delta t = 5\text{E-}1$

(c) $\delta t = 2.5\text{E-}1$

(d) REF

Figure 4: Solution for the linearized method applied on the pattern model (6) for $\chi = 12$ for successive δt. Other parameters chosen as in figure 3. The last subplot displays the reference solution as in figure 3. Note the negative values in the first three subplots.

coupled system dominates and eventually pollutes the solution. Thus in terms of efficiency, the monolithic approach is highly favorable. When comparing both alternatives of the monolithic approach we cannot recognize such a clear tendency. For large time steps we would prefer the Newton-like method while for moderate δt the higher accuracy of this method involves additional expenses for nonlinear iterations and assembly of the Jacobian. However we remark that a stronger coupling, in terms of higher values of χ, results in a better efficiency of the Newton-like method.

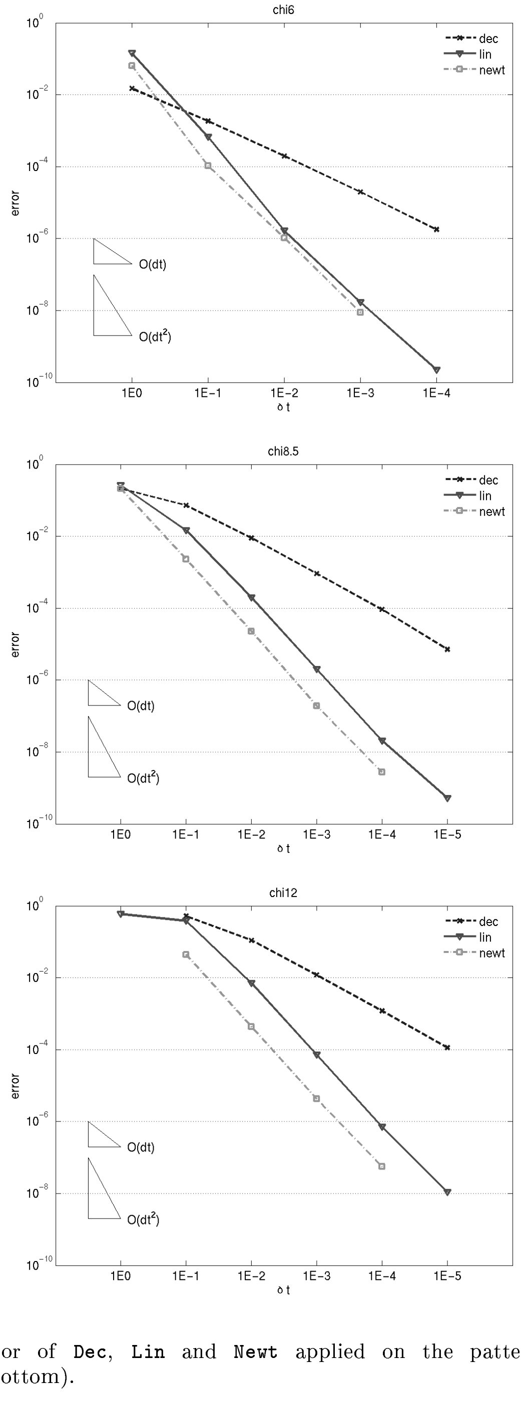

Figure 5: Relative error of `Dec`, `Lin` and `Newt` applied on the pattern model (6) for $\chi = 6$ (top) , 8.5 (mid) , 12 (bottom).

δ		`Dec`	`Lin`	`Newt`
1E-0	nonlin	28/80/47.8	-	6/10/7.4
	lin	27/30/28.0+23/31/25.6	108/122/115.2	168/316/211.5
5E-1	nonlin	17/42/25.8	-	4/6/4.3
	lin	26/27/26.6+17/23/18.6	73/85/78.2	95/121/109.1
2.5E-1	nonlin	13/25/15.4	-	3/4/3.4
	lin	24/28/25.7+11/17/12.5	49/64/57.5	55/84/68.4
1E-1	nonlin	8/14/9.3	-	3/4/3.0
	lin	21/24/23.0+9/14/10.6	35/47/39.6	38/69/49.1
5E-2	nonlin	6/10/7	-	2/3/2.1
	lin	16/19/18.4+11/19/14.5	33/45/35.2	34/62/42.8
2.5E-2	nonlin	5/7/5.4	-	2/3/2.0
	lin	13/15/13.6+15/25/19.7	29/41/30.9	30/47/37.1
1E-2	nonlin	4/6/4.1	-	2/3/2.0
	lin	8/10/8.6+19/31/24.5	23/30/24.1	23/36/29.6
5E-3	nonlin	3/5/3.3	-	2/2/2
	lin	8/10/9.1+21/34/26.9	21/28/24.4	21/31/25.6
2.5E-3	nonlin	3/4/3.0	-	2/2/2
	lin	12/14/13.8+22/34/28.3	23/30/26.2	22/36/29.1
1E-3	nonlin	2/3/2.5	-	1/2/1.4
	lin	16/20/18.3+22/38/29.5	23/31/27.6	22/39/29.7
5E-4	nonlin	2/3/2.0	-	1/2/1.0
	lin	18/23/21.8+23/36/28.9	23/31/28.4	22/35/28.3
2.5E-4	nonlin	2/2/2.0	-	1/2/1.0
	lin	20/25/23.9+23/33/29.1	23/31/28.5	23/35/28.5
1E-4	nonlin	2/2/2.0	-	1/1/1.0
	lin	20/27/25.2+23/37/30.1	23/31/28.7	23/31/28.6
5E-5	nonlin	2/2/2.0	-	1/1/1.0
	lin	20/28/25.7+23/39/31.1	23/31/28.7	23/31/28.7
2.5E-5	nonlin	1/2/1.1	-	1/1/1.0
	lin	20/28/25.9+23/37/28.9	23/31/28.7	23/31/28.7
1E-5	nonlin	1/2/1.0	-	1/1/1.0
	lin	20/28/26.1+23/33/28.7	23/31/28.7	23/31/28.7

Table 4: Iterations needed per time step for the three approaches applied on the pattern model (6). Parameters as before, except $\chi = 8.5$. 'Nonlin' accounts for the minimal/maximal/average iterations of the nonlinear defect-correcting loop whereas 'lin' accounts analogously for the iterations of the linear sub-problem per nonlinear step. In the case of `Dec` we list the iterations for c and u, separated via $+$.

5. Discussion and outlook

We presented three different numerical approaches for models of chemotaxis and quantitatively exposed their applicability to those models by numerical simulations. The analysis of our observations leads to the conclusion that highly efficient, accurate and flexible FE solvers are necessary to treat models of chemotaxis. The Newton-like scheme provides the most reliable solutions for large time steps, whereas the decoupled and linearized alternatives offer rather poor results, particularly for a dominant chemosensitivity. For a small time stepping we observe a similar quantitative behavior for both monolithic approaches. The straightforward decoupled scheme may only be favored in the presence of a weak coupling or a moderate chemosensitivity, since in this context its poor accuracy can be countered by the low computational costs.

Let us come back to an issue that we considered only slightly in this paper, but which is worth for discussion. When returning back to the Newton-like method presented in section 3.3.1 we remark that there are still enough untouched topics for further investigations, which aim at the enhancement of flexibility/robustness (and to a certain extend, efficiency as well). We have already mentioned some possible extensions to our basic Newton-like method. The main issue of a pure Newton scheme is its (only) local convergence. Thus the aim of a well elaborated Newton-like method is to reach the region of convergence with as few as possible nonlinear iterations. So called global Newton-like methods use a damping factor $\lambda \in (0, 1]$ in front of the Newton-updates y in equation (15). The idea is to damp the updates correspondingly to their distance to the (unknown) solution. A valuable damping-strategy applies a damping factor $0 < \lambda << 1$ on iterates that are far away from the solution and increases it to $\lambda \approx 1$ when the iterates approach the (initial) region of convergence, e.g. the solution. The choice of a suitable damping strategy is a crucial task and depends on the nonlinearity of the underlying PDE and the additional computational costs that we are ready to invest. The variety of damping strategies reaches from successively guessing a reasonable damping factor (e.g. cf. Armijo in [2]) up to pre-computing it via a thorough analysis of characteristics of the solution (e.g. cf. Deuflhard in [7]).

Since the present work only represents a first glance on efficient, accurate and flexible FE solvers for chemotaxis problems, let us furthermore give an outlook for promising further studies.
Nowadays, modern FE-solvers use multigrid algorithms, adaptive temporal and spatial meshes to come up with a solver that flexibly adopts to the governing discrete system of PDEs. These methods likely promise an even more efficient computation of chemotaxis models, because chemotactical dynamics may rather occur locally than globally on the whole temporal and spatial mesh.
Secondly we notice that we did not incorporate stabilization techniques, which are essential for ill-conditioned systems (or at least potentially extinguish numerical noise). When considering PDE systems which exhibit severe instabilities, e.g. negative solution values or highly oscillatory behavior, stabilization techniques are obviously very favorable. As Strehl et al. already documented in [26] and [27] a stabilization via Algebraic Flux Correction (AFC), cf. Kuzmin and Möller in [16], indeed works very well. Although Strehl et al. have only studied the decoupled approach there is strong evidence that a

Newton-like scheme for chemotaxis models can benefit from an AFC-like stabilization technique, e.g. Möller successfully applied a Total Variation Diminishing (TVD) scheme on a Newton-like method for a hyperbolic system in [18]. Since our underlying chemotaxis models are of mixed parabolic-hyperbolic type and incorporate additional sources and sinks (growth and decay terms) ongoing investigations for a suitable stabilization of AFC/TVD type provide a desirable and promising challenge for future work.

Acknowledgements

Robert Strehl is supported by a scholarship of the TU Dortmund.

References

[1] M. Aida, T. Tsujikawa, M. Efendiev, A. Yagi, M. Mimura, *Lower estimate of the attractor dimension for a chemotaxis growth system*, J. London Math. Soc. **74** (2006), no. 2, pp. 453–474.

[2] L. Armijo, *Minimization of functions having Lipschitz continuous first partial derivatives*, Pacific Journal of Mathematics **16**, no.1 (1966), pp. 1–3.

[3] R. Barrett, M. Berry, T. F. Chan, J. Demmel, J. M. Donato, J.Dongarra, V. Eijkhout, R. Pozo, C. Romine, H. Van der Vorst, *Templates for the Solution of Linear Systems: Building Blocks for Iterative Methods*, SIAM (1994).

[4] A. Chertock, A. Kurganov, *A second-order positivity preserving central-upwind scheme for chemotaxis and haptotaxis models*, Numer. Math. **111** (2008), pp. 169–205.

[5] S. Childress, *Chemotactic collapse in two dimensions*, Lecture Notes in Biomathematics, Springer-Verlag **55** (1984), pp. 61–66.

[6] S. Childress, J.K. Percus, *Nonlinear aspects of chemotaxis*, Math. Biosc. **56** (1981), pp. 217–237.

[7] P. Deuflhard, *Newton Methods for Nonlinear Problems, Affine invariance and adaptive algorithms*, Springer Series in Computational Mathematics **35** (2006) .

[8] Y. Epshteyn, *Discontinuous Galerkin methods for the chemotaxis and haptotaxis models*, J. Comput. Appl. Math. **224** (2009), no. 1, pp. 168–181.

[9] Y. Epshteyn, A. Kurganov, *New interior penalty discontinuous Galerkin methods for the Keller-Segel chemotaxis model*, SIAM J. Numer. Anal. **47** (2008), no. 1, pp. 386–408.

[10] F. Filbet, *A finite volume scheme for the Patlak-Keller-Segel chemotaxis model*, Numer. Math. **104** (2006), no. 4, 457–488.

[11] M. Gerber, R. Span, *An Analysis of Available Mathematical Models for Anaerobic Digestion of Organic Substances for Production of Biogas*, proc. IGRC, Paris (2008)

[12] D. Horstmann, *From 1970 until present: The Keller-Segel model in chemotaxis and its consequences I*, Jahresberichte der DMV **105** (2003), pp. 103–165.

[13] E. F. Keller and E. F. Segel, *Initiation of slime mold aggregation viewed as an instability*, J. Theor. Biol. **26** (1970), pp. 399–415.

[14] E. F. Keller and E. F. Segel, *Model for chemotaxis*, J. Theor. Biol. **30** (1971), pp. 225–234.

[15] B. S. Kirk, G. F. Carey, *A parallel, adaptive Finite Element scheme for modeling chemotactic biological systems*, Commun. Numer. Meth. Engng. **00** (2000), 1–6.

[16] D. Kuzmin and M. Möller, *Algebraic flux correction I. Scalar conservation laws*, in: D. Kuzmin, R. Löhner, S. Turek (eds), *Flux-Corrected Transport: Principles, Algorithms, and Applications*, Springer, Berlin (2005), pp. 155–206.

[17] M. Mimura, T. Tsujikawa, *Aggregating pattern dynamics in a chemotaxis model including growth*, Physica A, **230** (1996), pp. 499–543.

[18] M. Möller, *Adaptive high–resolution finite element schemes*, Doctoral dissertation, Technische Universität Dortmund, (2008).

[19] M. R. Myerscough, P. K. Maini, K. J. Painter, *Pattern formation in a generalized chemotaxis model*, Bull. of Math. Biol. **60** (1998), pp. 1–26.

[20] T. Nagai, T. Senba, K.Yoshida, *Application of the Trudinger-Moser Inequality to a Parabolic System of Chemotaxis*, Funkcialaj Ekvacioj **40** (1997), pp. 411–433.

[21] V. Nanjundiah, *Chemotaxis, signal relaying and aggregation morphology*, J. Theor. Biol. **42** (1973), pp. 63–105.

[22] K. J. Painter, T. Hillen, *Spatio-temporal chaos in a chemotaxis model* Physica D **204** (2011), pp. 363–375.

[23] K. J. Painter, T. Hillen, *Volume-filling and Quorum-sensing in models for chemosensitive movement*, Canadian Applied Mathematics Quarterly **10**(4) (2002), pp. 501–543.

[24] C. S. Patlak, *Random walk with persistence and external bias*, Bull. Math. Biol. Biophys. **15** (1953), pp. 311–338.

[25] L. Segel, *A theoretical study of receptor mechanisms in bacterial cemotaxis*, SIAM J. Appl. Math., **32** (1977), pp. 653–665.

[26] R. Strehl, A. Sokolov, D. Kuzmin, S. Turek, *A flux-corrected finite element method for chemotaxis problems*, CMAM **10** (2010), no. 2, pp. 118–131.

[27] R. Strehl, A. Sokolov, D. Kuzmin, D. Horstmann, S. Turek, *A positivity-preserving finite element method for chemotaxis problems in 3D*, TU Dortmund, preprints (2011).

[28] J. I. Tello and M. Winkler, *A Chemotaxis System with Logistic Source*, Comm. Partial Diff. Eqns **32** (2007), pp. 849–877.

[29] S. Turek, *A comparative study of some time-stepping techniques for the incomressible Navier-Stokes equations: From fully-implicit nonlinear schemes to semi-implicit projection methods*, Int. J. Num. Meth. Fluids, **22**, no. 10, (1996), pp. 987–1011.

[30] R. Tyson, L. G. Stern, R. J. LeVeque, *Fractional step methods applied to a chemotaxis model*, J. Math. Biol. **41** (2000), pp. 455–475.